Al–Fe^{3+} and Ca–Sr^{2+} epidotes in metagreywacke-quartzofeldspathic schist, Southern Alps, New Zealand

RODNEY GRAPES AND TERUO WATANABE[1]

Joint Mineral Sciences Research Laboratory
Victoria University of Wellington, New Zealand

Abstract

Al–Fe^{3+} and Sr^{2+}-bearing epidotes are a common constituent in chlorite and biotite–albite zone metagreywacke–quartzofeldspathic schist in the Southern Alps of New Zealand. On the basis of electron microprobe backscattered electron scanning of complexly zoned grains five generations of epidote growth are recognized. First generation epidotes (Ps$_{29-25}$) are typically fractured as a result of cataclasis during D$_1$ deformation and presumably represent relics of prehnite–pumpellyite and/or pumpellyite–actinolite facies conditions of metamorphism. Second generation epidote (Ps$_{25-20}$) rims first generation epidote and replaces fragmented grains. Third generation epidote involved Sr-replacement, up to 8.5 wt.% SrO, of earlier grains along fracture planes and grain margins. Single grains exhibit a range of Sr $\rightleftharpoons$ Ca replacement that can vary by up to 4 wt.% SrO. Fourth generation (post D$_1$) epidote (Ps$_{20-9}$) occurs as overgrowths on earlier generation epidotes and as continuously zoned grains. Within the lowest grade part of the biotite–albite-oligoclase zone fourth generation epidote cores (Ps$_{10-13}$) are overgrown by slightly more Fe-rich fifth generation rims (Ps$_{16-14}$) suggesting involvement of the epidote Ca$_2$Al$_3$Si$_3$O$_{12}$(OH) component in an oligoclase-producing reaction. In quartzofeldspathic lithologies epidote disappears at higher grades than the appearance of oligoclase.

Epidote compositions plot within the miscibility gap defined by Raith (1976) and a discontinuity between compositions of Ps$_{20}$ and Ps$_{16}$ in chlorite zone rocks is attributed to the persistence of relic cores due to incomplete Fe^{3+} $\rightleftharpoons$ Al diffusional exchange at low temperature and textural grade. With increasing grade there is a decrease in the range of zoning in individual epidote grains resulting in a more homogeneous population of epidote compositions with the most Al-rich epidotes becoming Fe^{3+}-rich and the most Fe^{3+}-rich epidotes becoming more Al-rich. The formation of Sr-epidote appears to be related to the release of Sr into the fluid phase from the breakdown of detrital plagioclase over the pumpellyite-clinozoisite isograd during D$_1$ deformation. Early-formed oligoclase in the biotite–albite–oligoclase zone resulting from the disappearance of epidote contains up to 0.4% SrO. Mobility of Sr (and Ca) is indicated by veins containing Sr-bearing epidote and calcite. The complex zoning of epidotes is a function of bulk composition, time, variation in fluid composition, temperature, pressure and deformation of the rocks.

Introduction

Minerals of the clinozoisite (Ca$_2$Al$_3$Si$_3$O$_{12}$(OH))-pistacite (Ca$_2$Fe$_3$Si$_3$O$_{12}$(OH)) series have been extensively studied in rocks ranging in grade from greenschist to amphibolite facies (e.g., Strens, 1964; Holdaway, 1965; Brown, 1967; Cooper, 1972; Hörmann and Raith, 1973; Hietanen, 1974; Raith, 1976). Nearly all petrological studies to date relate to epidote paragenesis in metabasic rocks. These studies are supported by experimental work (Holdaway, 1972; Liou, 1973) which find that oxygen fugacity and bulk composition exert important controls on epidote composition. Consequently, epidotes in metasedimentary or carbonate rocks associated with metabasites of the same grade may be expected to show significant differences in their paragenesis, compositional ranges, reactions and stability. This paper examines the relationship between epidote composition and paragenesis in the transition from metagreywacke to schist in the Southern Alps of New Zealand. Because of variable and complex zonal relationships exhibited by the epidotes, compositional mapping of individual grains using backscattered electron scanning was used to determine their

growth history and relate this to the metamorphic chronology of the rocks studied.

Regional setting, bulk composition and mineral assemblages

Epidote-bearing metasediments and schists were collected from the upper reaches of the Franz Josef and Fox Glacier Valleys, central part of the Southern Alps, South Island of New Zealand. The samples extend from the pumpellyite–clinozoisite isograd near the Main Divide of the Alps westward through the chlorite, biotite–albite and biotite–albite–oligoclase zones towards the Alpine Fault (Grapes and Otsuki, 1983). Following the scheme proposed by Bishop (1972) to describe a metagreywacke-schist transition in the Dansey Pass area of North Otago, this sequence can be conveniently subdivided into a series of textural zones that represent the transition from weakly schistose metagreywacke to laminated quartzo-feldspathic schists over a structural thickness of some 7 km.

Structural and mineralogical evidence indicates that the rocks have been subjected to an early (D_1) deformation which becomes increasingly more penetrative westwards with the development of a schistosity (S_1) in the higher grade part of the biotite–albite zone that is essentially parallel to original sedimentary bedding. A second schistosity (S_2) is parallel to the axial planes of the large km scale (F_2) folds in the area. It forms an axial plane cleavage in rocks of chlorite and biotite-albite zones but in the biotite-albite-oligoclase rocks forms a well-developed schistoxity that transposes and may obliterate S_1.

Apart from minor amounts of metabasite and metachert, the dominant lithology in the Alpine terrane is greywacke-argillite or their quartzofeldspathic schist equivalents. Bulk compositions are limited between SiO_2 64.6–69.7%; Al_2O_3 14.0–18.3%; Fe_2O_3 0.6–1.9%; FeO 1.6–4.2%; MgO 1.2–2.4%; CaO 1.9–3.2%; Na_2O 2.2–4.3%; K_2O 2.0–4.6% (Grapes et al., 1982). Sr contents vary between 476 and 283 ppm (average of 398 ppm) in chlorite and biotite–albite zone metagreywackes and semischists. In biotite–albite–oligoclase schists Sr averages 219 ppm. Oxidation ratios (mol.% $100 \times 2Fe_2O_3/(2Fe_2O_3+FeO)$) range from 50.0 to 24.6 in chlorite and biotite-albite zone rocks and decrease to 16.0 over the oligoclase-in isograd with the development of textural zone 4 schists. The Fe_2O_3/Al_2O_3 ratio varies between 0.13 and 0.10 in chlorite and biotite–albite zone rocks and, like the oxidation ratio, drops to 0.05 or below in those of the biotite–albite–oligoclase zone.

Detrital and authigenic mineral assemblages in the rocks are given in Table 1. At higher grades (i.e., garnet zone) epidote is only rarely found in the quartzofeldspathic schists and its presence is largely a function of relatively higher bulk Fe_2O_3/Al_2O_3 ratios. In metabasic horizons, however, epidote persists into the (staurolite)–oligoclase zone representing amphibolite facies grade (Cooper, 1972).

Analytical method

Epidote analyses were made on carbon-coated thin sections using an automated JEOL 733 electron microprobe. Accelerating voltage was 15 kV with a specimen current of 1.2×10^{-8}A and a beam diameter of 2–3 μm. Synthetic and natural mineral standards were used (Watanabe et al., 1981). Correction for dead time, background and current drift were applied before wt.% oxides were calculated using the method of Bence and Albee (1968). Alpha factors are those of Albee (pers. comm.) or Nakamura and Kushiro (1970). Grain homogeneity and analyzing positions were determined using backscattered electron imaging (BEI) in all cases.

Epidote composition

Bulk variation

Epidote composition (expressed as pistacite (Ps) content = $100 \times Ca_2Fe_3Si_3O_{12}(OH)$) from the pumpellyite–clinozoisite isograd to the lower-grade part of the biotite–albite–oligoclase zone is given in Figure 1. The large spread of epidote Ps contents is mainly due to the presence of several generations of epidote within the rocks (described in more detail below). With increasing metamorphic grade this compositonal range diminishes with progressive Fe^{3+} enrichment of the most Al-rich epidotes and, to a lesser extent, Al-enrichment of the most Fe^{3+}-rich epidotes. The iron enrichment of the most Al-rich epidotes with increasing grade is consistent with a similar trend shown by the clinozoisite limb of the zoisite–clinozoisite solvus documented by Enami and Banno (1980). Above the oligoclase-in isograd epidote compositions are decidedly more aluminous (Fig. 1).

In chlorite zone rocks no epidotes with Ps contents between Ps_{20} and Ps_{16} have been found whereas in the biotite–albite and biotite–albite–oligoclase zone rocks epidote compositions occupy this gap. Epidotes in lowest grade chlorite zone quartzofeldspathic schists in the Dansey Pass area, North Otago (Bishop, 1972) contain a similar hiatus between Ps_{21} and Ps_{13-14} as do epidotes in rocks of the same grade elsewhere in the Haast schist terrane, e.g., Brown (1967); Kawachi (1975). Below the pumpellyite–clinozoisite isograd, i.e., in pumpellyite–actinolite facies metagreywackes, epidote compositions are $>Ps_{20}$ (see also Bishop, 1972 and Kawachi, 1975). Such gross compositional shifts support the suggestion of Miyashiro and Seki (1958) that iron-rich epidotes form early or at low temperatures and become more aluminous with increasing temperature. In detail, however, rock chemistry, oxidation ratio, and fluctuations in fluid composition are probably more important than temperature in affecting Al $\rightleftharpoons Fe^{3+}$ substitution in epidote.

Zoning and replacement relations

Core-rim and replacement relations displayed by heterogeneous epidote grains (Fig. 2) indicate that, with the

Table 1. Mineral distribution in chlorite–biotite zone metagreywacke–quartzofeldspathic schist, Franz Josef-Fox Glacier area, Southern Alps, New Zealand.

Sample No.	724	620	723	621 625/6 628 631	636 725 639	991 992	993
Textural Zone (see below)		2A		2B	3A	3B	4
Zone	Pumpellyite-actinolite zone	Chlorite zone		Biotite-albite zone			Biotite-albite oligoclase zone
Facies	Pumpellyite-actinolite facies	Greenschist					Transitional

Detrital Minerals

Quartz
Plagioclase
K-feldspar
Fe^{3+}-Epidote
Al-Epidote
Allanite
Muscovite
Biotite
Chlorite
Hornblende
Zircon
Apatite
Graphite
Ilmenite

Authigenic Minerals

Quartz
Albite
Oligoclase
Epidote
Clinozoisite
Pumpellyite
Actinolite
Chlorite
Biotite
Phengite
Stilpnomelane
Carbonate
Tourmaline
Sphene
Ilmenite
Sulphide

Vein Minerals

Quartz
Adularia
Pumpellyite
Epidote
Chlorite
Carbonate

Textural Zone nomenclature after Bishop (1972); 2A - weakly schistose fissile greywacke with axial plane cleavage penetrative on microscope scale; 2B - semischist with penetrative foliation down to microscope scale; 3A - semischist with weakly developed quartz-albite rich segregation lamellae; 3B - distinctly laminated schists with segregation lamellae <2mm thick; 4 - schist with segregation lamellae >2mm thick.

exception of detrital epidote and allanite, there are four generations of epidote growth/replacement in most of the rocks examined. A fifth generation of epidote is found in schists of the biotite–albite–oligoclase zone.

Detrital grains are recognized by their smoothed subrounded outlines and typically coarse grain size. Most grains are Fe-rich ($Ps_{>30}$) although rare grains of $Ps_{13–14}$ have been found in one metagreywacke (No. 724) near the pumpellyite–clinozoisite isograd. Lithic fragments and detrital minerals indicate that the New Zealand greywackes were derived from a granitic-gneissic terrane (e.g., Reed, 1957). Although epidotes (both magmatic and

hydrothermal) are typically Fe-rich in such rocks (e.g., Tulloch, 1979; Dickin et al., 1980), the restricted Ps range ($Ps_{30–33}$) of the detrital Fe-rich epidotes in the rocks of the present area could be the result of compositional adjustment during subsequent prehnite–pumpellyite or zeolite facies metamorphism. Partial microprobe analysis of detrital allanite indicates that it is an Mg-rich variety with up to 4.2% MgO.

The earliest *authigenic* epidote recognized is also Fe-rich and has compositions ranging from $Ps_{29–25}$. It occurs as individual grains (chlorite zone), as cores (biotite–albite zone), and as overgrowths on detrital epidote and
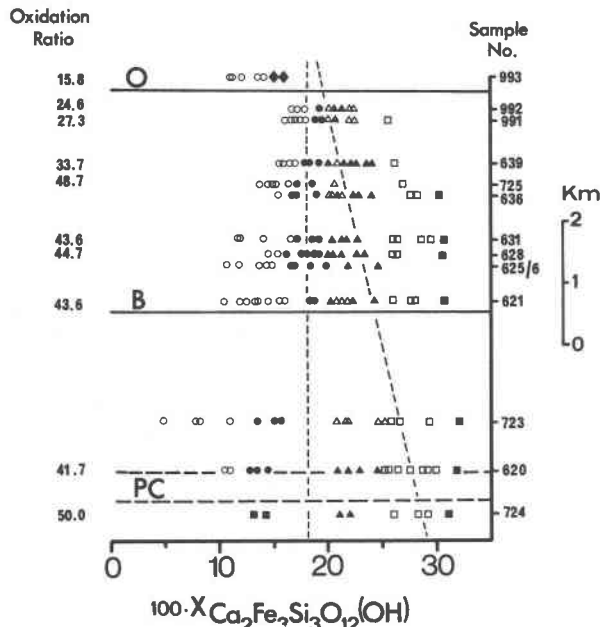
Fig. 1. Epidote compositions, $100 \times Ca_2Fe_3Si_2O12(OH)$, plotted against distance measured approximately normal to dip and strike of mineral isograds, Franz Josef-Fox Glacier area. PC = pumpellyite–clinozoisite isograd. B = biotite isograd. O = oligoclase isograd. Symbols: ■ Detrital epidote; □ First generation cores or rims around detrital epidote and/or allanite; ▲ Second generation cores or replacement rims around first generation grains, detrital epidote and/or allanite; △ Third generation Sr-rich epidote replacing second generation epidotes; ● Fourth generation rims around first, second and third generation epidote or ○ weakly zoned or homogeneous grains; ◆ Fifth generation rims around fourth generation grains (only in biotite–albite–oligoclase zone). Dashed lines refer to position of the inferred miscibility gap given by Raith (1976).

allanite. Many grains (>80 μm diameter) of this generation, especially those in biotite–albite samples, have been extensively fractured and are often fragmented by cataclasis that accompanies the transition from metagreywacke to schist (Figs. 2b,c). Such a textural relationship indicates that these epidotes formed prior to the development of the weak S_1 foliation. They presumably represent *relics of a lower grade of metamorphism*, perhaps equivalent to pumpellyite–actinolite or even prehnite–pumpellyite facies grade. Epidotes of a similar composition have been analyzed by Brown (1967) as relic cores in chlorite zone rocks of east Otago and by Kawachi (1975) in pumpellyite–actinolite facies pelitic rocks of the upper Wakatipu area, western Otago.

Second generation epidote, with compositions between Ps_{25} and Ps_{20}, occurs as both replacement rims and sharply defined overgrowths on first generation epidote, and as discrete, homogeneous to weakly continuously zoned grains with rims enriched in Al. Where extensive fragmentation of first generation epidote has occurred,

nearly total replacement of the smaller fragments by second generation epidote has taken place.

The third generation of epidote is characterized by significant amounts of SrO, which is detailed below. Sr-rich epidote shows up clearly as bright areas on backscattered electron scanning images and in chlorite and biotite–albite zone rocks it denotes a distinctive time and composition marker between first, second and fourth generation epidotes (Fig. 2a,b,c,d,e). Sr-rich epidote replaces previously formed epidote around margins and along fracture planes. Depending on the generation of epidote that is being replaced, Sr-epidote compositions fall within two groupings of Ps_{29-25} and Ps_{25-20}. Smaller grains in the upper grade part of the biotite–albite zone (e.g., Fig. 2e), often exhibit a diffuse contact between areas of Sr-enrichment and overgrowths of fourth generation epidote suggesting that a limited amount of Sr-replacement of these overgrowths occurred after they had formed. In the biotite–albite–oligoclase zone, Sr-epidote may occur as narrow rims on fourth generation epidote of Ps_{11-13} (Fig. 2f).

Epidotes of the fourth generation mantle first and second generation grains and also typically enclose third generation Sr-epidote replacement rims and grains. Compositions vary from Ps_{15-6} in chlorite zone rocks and from Ps_{20-9} and $Ps_{20-16.5}$ in the lower and higher grade rocks of the biotite–albite zone respectively (Fig. 1). Small (<10 μm), homogeneous grains of this generation are always the most Al-rich in any one sample, but otherwise compositional variation in fourth generation epidotes is due to a continuous zoning from Fe-rich cores to Al-rich rims. Overgrowths on earlier formed epidote tend to be relatively homogeneous. In the lowest grade rocks of the biotite-albite-oligoclase zone, the epidotes are notably more aluminous (Fig. 1) with cores of Ps_{10-11} *gradationally* zoned by compositions up to Ps_{13}, the reverse trend of that in lower grade rocks.

In the biotite–albite zone, overgrowths of fourth generation, and rarely second generation epidote, characteristically have well developed crystal outlines and are often poikiloblastic (e.g., Fig. 2d). This habit suggests that they are post S_1 which fragmented the larger grains of earlier generations.

Fourth generation Al-rich epidote (<Ps_{15}) is first found in the vicinity of the pumpellyite-out–clinozoisite-in isograd and is accompanied by a decrease in modal chlorite and increasing amounts of actinolite suggesting a pumpellyite consuming reaction leading to a greenschist facies assemblage such as, pumpellyite + chlorite + quartz = actinolite + clinozoisite + H_2O (Banno, 1964).

The continuous nature of this reaction has led to a degree of uncertainty in determining the position of this isograd. Expansion of the range of epidote composition across the pumpellyite–clinozoisite isograd "zone", especially with regard to the minimum Ps content (cf. Nakajima et al., 1977) results in the appearance of clino-
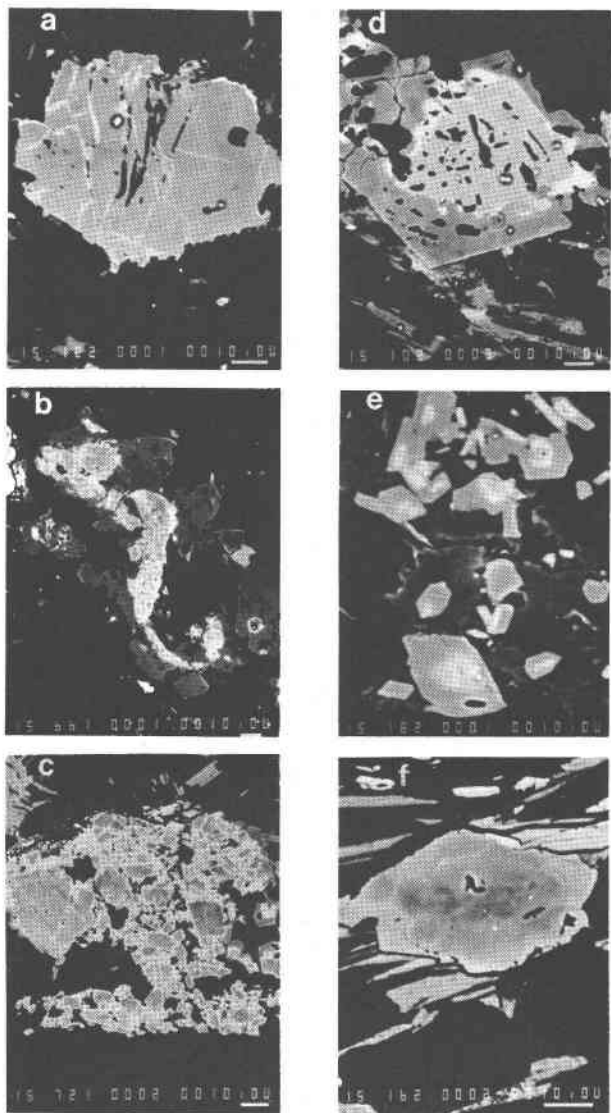
Table 2. Representative analyses and formulae on the basis of 12.5 (O) of Sr-epidotes, Franz Josef-Fox Glacier area, Southern Alps, New Zealand.

Sample No.	725		723
SiO_2	37.67	36.72	36.67
Al_2O_3	25.27	24.37	23.06
Fe_2O_3*	10.12	11.13	12.24
MnO	0.00	0.00	0.00
CaO	22.78	19.96	18.65
SrO	2.13	5.73	8.36
H_2O(calc)	1.88	1.84	1.83
Total	99.94	99.79	100.86
Si	3.014	2.984	2.999
Al	2.366	2.334	3.223
Fe^{3+}	0.599	0.680	0.753
Σ (M)	2.965	3.014	2.976
Ca	1.832	1.738	1.634
Sr	0.180	0.270	0.397
Σ (A)	2.012	2.008	2.031

*All iron as Fe_2O_3

zoisite (Ps <10) some distance upgrade of the approximate position of the isograd (Fig. 1).

Above the oligoclase isograd, which more or less coincides with the development of >2mm thick quartz-plagioclase and mica-rich laminae (textural zone 4), fourth generation epidotes have their long axes oriented parallel to the lamellae. Fifth generation optically discontinuous rims (Ps_{14-16}) typically extend these grains in the direction of the schistosity (Fig. 2f) which implies that they grew during S_2 development. Iron enrichment of the epidote rims coincides with the incoming of small amounts of oligoclase (An_{20-24}) (Grapes and Otsuki, 1983) and an abrupt decrease in the modal amount of epidote. Such a relationship suggests a reaction where the Ca_2Al_3 $Si_3O_{12}(OH)$ component of epidote is selectively consumed to form the anorthite molecule in plagioclase which would result in concomitant iron enrichment of the reactant epidote through a reaction such as

Fig. 2. Backscattered electron scanning photos of epidotes, Franz Josef-Fox Glacier area. Bar scale = 10 μm. (a) First generation epidote (Ps_{28}) showing Sr-replacement (white) along cracks (No. 723, chlorite zone). (b) Disrupted and intensely fractured first generation epidote (Ps_{27-28}) with extensive Sr-replacement (white areas) along fractures, surrounded by a spongy overgrowth of fourth generation epidote (darker grey of Ps_{16}). Weakly developed S_1 schistosity in the section runs diagonally across the photo parallel to the elongation of the fractured first generation epidote (No. 621, low grade part of the biotite-albite zone; Textural zone 2B). (c) Large grain of first generation epidote (Ps_{27}) (light grey) partially replaced by second generation epidote (Ps_{23-21}) (darker grey patches) that has been extensively fractured and disrupted. Cracks and fractured fragments have been rimmed and partially replaced by Sr-epidote (white) which in turn has been overgrown in places by fourth generation epidote (right side of photo) of Ps_{16} with euhedral outlines (No. 625, low grade part of biotite-albite zone; Textural zone 3A). (d) Euhedral overgrowth of fourth generation epidote (Ps_{18}) (grey) on second generation epidote (Ps_{22}) (light grey) partially rimmed by Sr-epidote (white). Mica flakes in lower part of photo define the S_1 schistosity (No. 725, biotite-albite zone; Textural zone 3A). (e) Small euhedral grains of fourth generation epidote (Ps_{18-19}) with cores of second generation epidote (Ps_{23-21}) largely replaced by Sr-epidote. Brighter areas contain greater amounts of SrO. In comparison with (d) boundaries between core and rim are diffuse. (No. 991, higher grade part of biotite-albite zone; Textural zone 3B). (f) Heterogeneous fourth generation epidote in mica-rich layer of quartzofeldspathic schist containing a core (dark grey) of Ps_{11} continuously zoned to Ps_{13} and overgrown by fifth generation epidote of Ps_{16} (lighter grey) elongated in the direction of the S_2 schistosity. The thin white rim marking the junction between fourth generation epidote and fifth generation overgrowth is enriched in SrO. The white areas along the outermost margins of the grain are the result of an edge effect. (No. 993, biotite-albite-oligoclase zone; Textural zone 4).
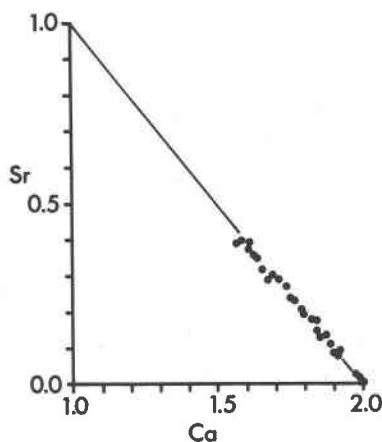
Fig. 3. Range of $Sr^{2+} \rightleftharpoons Ca^{2+}$ substitution in A(2) site of epidotes, Franz Josef-Fox Glacier area.

Epidote (Solid Solution) + muscovite + chlorite
$\quad$ + quartz = anorthite component of plagioclase
$\quad$ + Fe-richer epidote + biotite + H_2O. $\qquad$ (1)

Sr-content of epidote

As stated above, Sr-bearing epidotes were only revealed by backscattered electron scanning where they show up as bright areas from the grey tones of Fe–Al epidote. Microprobe analyses (Table 2) indicate SrO contents ranging from 0.10 to 8.5 wt.% with the degree of BEI brightness intensifying as SrO content rises. Representative analyses of Sr-bearing epidotes are given in Table 2. According to Dollase (1971) Sr should replace Ca only in the A(2) site of the epidote structure and Figure 3 indicates that up to 40% of this site is occupied by Sr^{2+} in epidotes of this study. In most cases single epidote grains exhibit a range of $Sr \rightleftharpoons Ca$ replacement that can vary by as much as 4 wt.% SrO. Variation of SrO in epidotes with respect to metamorphic grade is shown in Figure 4. Near the pumpellyite–clinozoisite isograd, epidote SrO content is below 2 wt.% and rapidly increases to a maximum of 8.5% in epidotes of the chlorite zone (No. 723) and maintains high concentrations of up to 7% in those of the biotite–albite zone. SrO contents of epidotes in schists of the biotite–albite–oligoclase zone are below 2.3%.

Sr-bearing epidotes and piemontite have only been rarely reported. A Pb–Sr epidote (hancockite) with 3.81% SrO have been analyzed from a pegmatite, Franklin, New Jersey, by Palache (1933). Hutton (1940) records a piemontite with 1.23% SrO from a manganiferous quartzose schist from northwest Otago. More recently, Schreyer and Abraham (1978) have analyzed epidotes with between 0.18 and 0.70% SrO in a metatonalite from the Venn-Stavelot Massif, Belgium. The Alpine Sr-epidotes are therefore the most Sr-rich reported to date and their discovery indicates that they are probably widespread throughout the low grade metagreywacke-quartzofeldspathic schist lithology of the Torlesse and Haast schist terranes. The well known enrichment of Sr in greenstones

dominated by epidote (e.g., Melson et al., 1968; Humphris and Thompson, 1978) suggests that Sr-rich epidotes may also be present in the associated metabasite horizons.

Mn-content of epidote

MnO contents are variable and in most epidotes range from 0.10 to 0.30 wt.%. There is no systematic change in epidote MnO contents with grade but within any one rock more Fe-rich grains have higher MnO than later generation Al-rich epidotes. Highest MnO contents (typically >0.6%) are recorded in detrital grains. In Sr-bearing epidote MnO is either absent or only present in minor amounts (<0.05 wt.%).

Discussion

Effect of host rock composition

In addition to $T–P$ conditions of metamorphism, fo_2 and bulk composition, particularly the oxidation and Fe_2O_3/Al_2O_3 ratios, control the maximum Fe^{3+} content of epidote (e.g., Holdaway, 1972; Cooper, 1972; Liou, 1973; Hörmann and Raith, 1973; Raith, 1976).

Oxidation ratios typically decrease with increasing metamorphic grade (e.g., Miyashiro, 1964), as in the present area (Fig. 1). There is a gradual overall decrease in the maximum Fe^{3+} content of epidotes, especially those in rocks of the biotite–albite–oligoclase zone where oxidation ratios <20 and Fe_2O_3/Al_2O_3 ratios are low (e.g.,
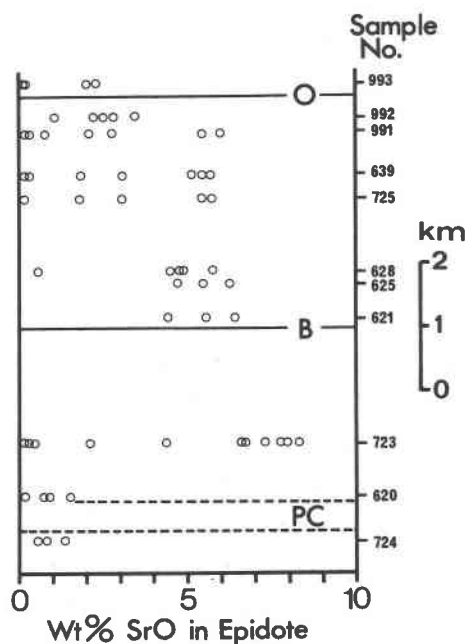

Fig. 4. Plot of wt.% SrO content of epidotes versus metamorphic grade, Franz Josef-Fox Glacier area. PC = pumpellyite–clinozoisite isograd; B = biotite isograd; O = oligoclase-in isograd.

No. 993, Fig. 1). Hematite and/or magnetite are absent in the samples studied and the opaque phases in the chlorite and biotite–albite zone rocks are pyrite and detrital ilmenite. Authigenic ilmenite first appears near the oligoclase-in isograd (Table 1). Minor amounts of graphite occur in all the rocks which indicates that fo_2 during metamorphism was low. These data are consistent with the maximum iron-enrichment of Ps_{25} for second and fourth generation epidotes (cf. Liou, 1973) and underscores the conclusion that epidotes with $Ps>25$ in the same rocks (Fig. 1) are relics of a lower metamorphic grade. On a more localized scale, the continuous zoning in single generation epidotes to more Al-rich compositions may, in part, record gradually decreasing fo_2 in the fluid phase with time under essentially isothermal/isobaric conditions (see also Bird and Helgeson, 1981). The decrease of rock Fe_2O_3/Al_2O_3 ratio from 0.13–0.10 in chlorite and biotite–albite zone rocks to values of 0.05–0.04 over the oligoclase-in isograd would explain the shift to more aluminous epidote compositions (Fig. 1).

Origin of Sr-bearing epidote

The occurrence of Sr-epidote as rims and fracture linings indicates increased aSr^{2+} in the fluid phase which resulted in hydrothermally-induced $Sr \rightleftharpoons Ca$ replacement of epidotes (the only major Ca-bearing phase present, Table 1) formed prior to or during the D_1 event. The most probable source of the strontium is detrital plagioclase which contains up to 0.24% SrO. Figure 4 indicates a significant increase in the extent of $Sr \rightleftharpoons Ca$ replacement in epidote over the pumpellyite–actinolite isograd which in this area coincides with extensive albitization and cataclastic reduction of detrital feldspar, suggesting that rapid Sr exchange between feldspar and fluid took place. With the breakdown of epidote over the oligoclase-in isograd, Sr is incorporated into newly-formed oligoclase. Oligoclase coexisting with epidote almost on the isograd has an SrO content of ~0.10–0.15% but with the complete disappearance of epidote, oligoclase contains higher values of ~0.3–0.4%. In associated calcite, strontium is below the detection limit, i.e., 0.07% SrO. The decrease in bulk rock Sr content and the range of $Sr \rightleftharpoons Ca$ substitution in epidotes over the oligoclase-in isograd, however, also suggests removal of some Sr (and Ca) in solution as indicated by vein epidote and calcite which in biotite–albite-zone rocks contain up to 0.48 and 0.38% SrO respectively. Sr mobility during greenschist facies metamorphism is also indicated by the occurrence of aragonite with 3.87% SrO in a vein cutting chlorite zone schists in the central Otago area of the Haast schist terrane (Hutton, 1936).

Effect of metamorphic grade

The complex zoning of greenschist facies epidotes provides a chronicle of successive stages of recrystallization of the rocks in the Franz Josef-Fox Glacier area.

Except in the biotite–albite–oligoclase zone where epidote was involved in a Ca-plagioclase forming reaction, the highest metamorphic grade attained is reflected by the most Al-rich epidote (fourth generation) rim and grain compositions. Iron-rich epidotes (first generation) formed prior to D_1 deformation presumably during prehnite–pumpellyite and pumpellyite–actinolite facies conditions. These grains were cataclasized and replaced in varying degrees to more aluminous compositions (second generation) during the development of S_1 and subsequently both generations were altered by $Sr \rightleftharpoons Ca$ metasomatism (third generation). The growth of fourth generation epidotes post-dated the D_1 phase during a relatively static interval of recrystallization. A subsequent higher temperature D_2 event resulted in the breakdown of epidote (reaction (1) above) to establish the oligoclase-in isograd.

Heterogeneous epidote grains indicate disequilibrium. At the low temperature and textural grade of the chlorite zone rocks the growth rate of fourth generation epidotes exceeded the rate of the intracrystalline exchange reaction $Fe^{3+}_{M(3)} + Al^{3+}_{M(1)} \rightleftharpoons Fe^{3+}_{M(1)} + Al^{3+}_{M(3)}$ (Bird and Helgeson, 1980) between these and earlier-generation epidotes that occur as cores, thus giving rise to the composition discontinuity recorded (Fig. 1). It is perhaps not surprising that composition gaps have frequently been recorded from greenschist and lower grade rocks elsewhere, e.g., Strens, 1964; Holdaway, 1965; Brown, 1967; Bishop, 1972; Hietanen, 1974; Raith, 1976, and have been used to support the presence of the miscibility gap in the clinozoisite–epidote series proposed by Strens (1965). There are, however, inconsistencies in the width and extent of such composition gaps and it is clear from Fig. 1 that many epidote compositions fall within the predicted miscibility gap delineated by Raith (1976), (see also Smith et al., 1982). The present data, therefore, do not support the presence of a miscibility gap under lower grade greenschist facies conditions of metamorphism (cf. Bird and Helgeson, 1980).

An increasing rate of Al–Fe³⁺ diffusion exchange with increasing temperature and textural grade development enabled a greater degree of individual grain homogenization to occur, especially in grains of 15 μm or less, as evidenced by the diffuse nature of core-rim contacts. This led to a decrease in the range of zoning with the disappearance of the lower-grade compositional gap and a more homogeneous population of epidote compositions, such as recorded in the highest grade part of the biotite–albite zone and in the biotite–albite–oligoclase zone (Fig. 1).

A similar effect is apparent in the extent of $Sr \rightleftharpoons Ca$ substitution in epidote. In chlorite zone metagreywacke epidotes, Sr replacement is localized along fracture planes. Within biotite–albite-grade samples more extensive replacement of first and second generation epidote occurs (Figs. 2b,c,d) and smaller fragments tend to be totally replaced (Fig. 2e). In such examples Sr decreases inward from the fracture/grain boundaries of first and

second generation epidotes or outwards into fourth generation rims suggesting the effect of a diffusion gradient. The amount of Sr replacement would presumably depend on the diffusion rate of Sr into epidote from the fluid phase and within the epidote itself, and this should increase with increasing temperature.

For a given bulk composition therefore, the tendency towards homogenization by $Al \rightleftharpoons Fe^{3+}$ exchange between the M(1) and M(3) sites and the extent of $Sr \rightleftharpoons Ca$ substitution in A(2)-site of earlier generation cores and later generation rims is a complex function of time, variation in fluid composition under isothermal/isobaric conditions, increasing temperature, pressure and deformation of the rocks.

References

Banno, S. (1964) Petrologic studies on Sambagawa crystalline schists in the Bessi-Ino district, central Sikoku, Japan. Journal of the Faculty of Science, University of Tokyo, Sec. II, 15, 203–319.

Bence, A. E. and Albee, A. L. (1968) Empirical correction factors for the electron microanalysis of silicates and oxides. Journal of Geology, 76, 382–403.

Bird, D. K. and Helgeson, H. C. (1980) Chemical interaction of aqueous solutions with epidote–feldspar mineral assemblages in geologic systems. I. Thermodynamic analysis of phase relations in the system $CaO-FeO-Fe_2O_3-Al_2O_3-SiO_2-H_2O-CO_2$. American Journal of Science, 280, 907–941.

Bird, D. K. and Helgeson, H. C. (1981) Chemical interaction of aqueous solutions with epidote-feldspar mineral assemblages in geologic systems. II. Equilibrium constraints in metamorphic geothermal processes. American Journal of Science, 281, 576–614.

Bishop, D. G. (1972) Progressive metamorphism from prehnite-pumpellyite to greenschist facies in the Dansey Pass area, Otago, New Zealand. Bulletin of the Geological Society of America, 83, 3177–3198.

Brown, E. H. (1967) The greenschist facies in part of eastern Otago, New Zealand. Contributions to Mineralogy and Petrology, 14, 259–292.

Cooper, A. F. (1972) Progressive metamorphism of metabasic rocks from the Haast Schist Group of southern New Zealand. Journal of Petrology, 13, 457–492.

Dickin, A. P., Exley, R. H. and Smith, B. M. (1980) Isotopic measurement of Sr and O exchange between meteroric-hydrothermal fluid and the Coire Uaigneich granophyre, Isle of Skye, N. W. Scotland. Earth and Planetary Science Letters, 51, 58–70.

Dollase, W. A. (1971) Refinement of the crystal structures of epidote, allanite and hancockite. American Mineralogist, 56, 447–464.

Enami, M. and Banno, S. (1980) Zoisite–clinozoisite relations in low- to medium-grade high-pressure metamorphic rocks and their implications. Mineralogical Magazine, 43, 1905–2013.

Grapes, R. H., Watanabe, T. and Palmer, K. (1982) X.R.F. analyses of quartzo-feldspathic schists and metacherts, Franz Josef-Fox Glacier area, Southern Alps of New Zealand. Department of Geology, Victoria University of Wellington, Publication No. 25.

Grapes, R. H. and Otsuki, M. (1983) Peristerite compositions in quartzofeldspathic schists, Franz Josef-Fox Glacier area, New Zealand. Journal of Metamorphic Petrology, 1, 47–61.

Hietanen, A. (1974) Amphibole pairs, epidote minerals, chlorite and plagioclase in metamorphic rocks, northern Sierra Nevada, California. American Mineralogist, 59, 22–40.

Holdaway, M. J. (1965) Basic regional metamorphic rocks in part of the Klamath Mountains, northern California. American Mineralogist, 50, 953–977.

Holdaway, M. J. (1972) Thermal stability of Al–Fe epidote as a function of fo_2 and Fe content. Contributions to Mineralogy and Petrology, 37, 307–340.

Hörmann, P-K. and Raith, M. (1973) Bildungsbedingungen von Al-Fe (III) Epidoten. Contributions to Mineralogy and Petrology, 38, 307–320.

Humphris, S. E. and Thompson, G. (1978) Trace element mobility during hydrothermal alteration of oceanic basalts. Geochimica et Cosmochimica Acta, 42, 127–136.

Hutton, C. O. (1936) Mineralogical notes from the University of Otago. Transactions of the Royal Society of New Zealand, 66, 35–37.

Hutton, C. O. (1940) Metamorphism in the Lake Wakatipu region, western Otago, New Zealand. New Zealand Department of Scientific and Industrial Research, Geological Memoir, 5.

Kawachi, Y. (1975) Pumpellyite–actinolite and contiguous facies metamorphism in part of upper Wakatipu district, South Island, New Zealand. New Zealand Journal of Geology and Geophysics, 18, 401–441.

Liou, J. G. (1973) Synthesis and stability relations of epidote, $Ca_2Al_2FeSi_3-OH_{12}(OH)$. Journal of Petrology, 14, 381–413.

Melson, W., Thompson, G. and Van Andel, T. H. (1968) Volcanism and metamorphism in the Mid-Atlantic Ridge, 22°N latitude. Journal of Geophysical Research, 73, 5925–5941.

Miyashiro, A. (1964) Oxidation and reduction in the Earth's crust with special reference to the role of graphite. Geochimica et Cosmochimica Acta, 28, 717–729.

Miyashiro, A. and Seki, Y. (1958) Enlargement of the composition field of epidote and piemontite with rising temperature. American Journal of Science, 256, 423–430.

Nakajima, T., Banno, S. and Suzuki, T. (1977) Reactions leading to the disappearance of pumpellyite in low-grade metamorphic rocks of the Sanbagawa metamorphic belt in central Shikoku, Japan. Journal of Petrology, 18, 263–284.

Nakamura, Y. and Kushiro, I. (1970) Petrology of some lunar crystalline rocks. Proceedings of the Apollo II Lunar Science Conference, I, 607–626.

Palache, C. (1936) Babingtonite and epidote from Westfield, Massachusetts. American Mineralogist, 21, 652.

Raith, M. (1976) The Al–Fe (III) epidote miscibility gap in a metamorphic profile through the Penninic Series of the Tauern

Window, Austria. Contributions to Mineralogy and Petrology, 57, 99–117.

Reed, J. J. (1957) Petrology of the Lower Mesozoic rocks of the Wellington district. New Zealand Geological Survey Bulletin, 57.

Schreyer, W. and Abraham, K. (1978) Prehnite/chlorite and actinolite/epidote bearing mineral assemblages in the metamorphic igneous rocks of La Helle and Challes, Venn-Stevelot Massif, Belgium. Annales de la Societe Geologique de Belgique, T, 101, 227–241.

Smith, R. E., Pedrix, J. L. and Parks, T. C. (1982) Burial metamorphism in the Hamersley Basin, Western Australia. Journal of Petrology, 23, 75–102.

Strens, R. C. J. (1964) Epidotes of the Borrowdale volcanic series of central Borrowdale. Mineralogical Magazine, 33, 868–886.

Strens, R. C. J. (1965) Stability relations of the Al–Fe epidotes. Mineralogical Magazine, 35, 464–475.

Tulloch, A. J. (1979) Secondary Ca–Al silicates as low-grade alteration products of granitoid biotite. Contributions to Mineralogy and Petrology, 69, 105–117.

Watanabe, T., Grapes, R. H. and Palmer, K. (1981) Quantitative analyses of rock forming minerals by JXA-733 electron probe X-ray microanalyser. JEOL News, 19E (1), 15–19.